

Holographic nature of critical quantum states of proteins

Eszter Papp and Gábor Vattay*
Department of Physics of Complex Systems
Institute for Physics and Astronomy
Eötvös Loránd University
H-1053 Budapest, Egyetem tér 1-3., Hungary
(Dated: July 23, 2024)

The Anderson metal-insulator transition is a fundamental phenomenon in condensed matter physics, describing the transition from a conducting (metallic) to a non-conducting (insulating) state driven by disorder in a material. At the critical point of the Anderson transition, wave functions exhibit multifractal behavior, and energy levels display a universal distribution, indicating non-trivial correlations in the eigenstates. Recent studies have shown that proteins, traditionally considered as insulators, exhibit much higher conductivity than previously assumed. In this paper, we investigate several proteins known for their efficient electron transport properties. We compare their energy level statistics, eigenfunction correlation, and electron return probability to those expected in metallic, insulating, or critical states. Remarkably, these proteins exhibit properties of critically disordered metals in their natural state without any parameter adjustment. Their composition and geometry are self-organized into the critical state of the Anderson transition, and their fractal properties are universal and unique among critical systems. Our findings suggest that proteins' wave functions fulfill "holographic" area laws, and the correlation fractal dimension is precisely $d_2 = 2$.

The Anderson metal-insulator transition[1] (MIT) is a fundamental phenomenon in condensed matter physics, describing the transition from a conducting (metallic) to a non-conducting (insulating) state driven by disorder in a material. As proposed by P.W. Anderson, this transition occurs due to the localization of electronic wave functions induced by random impurities or lattice defects. In a metallic phase, electrons can travel through the material as their wave functions are extended and correlated; random matrix theory[2, 3] describes the statistics of energy levels. However, as the disorder increases, these wave functions become increasingly localized, leading to an insulating state where eigenstates are spatially localized and uncorrelated; the energy levels follow Poisson statistics. The critical point of the Anderson transition is characterized by a unique set of properties where wave functions exhibit multifractal[4, 5] behavior. At the critical point, the level statistics deviate from the random matrix and Poisson distributions and instead display a universal distribution[6] that is intermediate between the metallic and insulating phases, highlighting the presence of non-trivial correlations in the eigenstates[7, 8]. The critical state has some peculiar features. For example, it has been argued[9, 10] that if one could artificially create a critically disordered metal in which the level of disorder is nearly perfectly adjusted to the critical point of the Anderson transition, a high temperature *fractal superconducting state* can arise due to the power-law dependence of the superconductor-insulator transition temperature on the interaction constant of the electron-electron attraction. It has also been found[11, 12] that systems near the critical point of MIT can have long coherence times and coherent transport at the same time, and some biological molecules prefer this state[13].

In the last ten years, measuring the conductivity of small-scale protein samples has become feasible. The previous belief that proteins are good insulators has been proven wrong; they exhibit much higher conductivity than previously assumed[14–16]. Protein conductance can occur over long distances[17] and in a temperature-independent manner[18] from four Kelvins to ambient temperatures, which is atypical for most conductive materials. In this study, we investigate several proteins known for efficient electron transport properties. We compare their energy level statistics, eigenfunction correlation, and electron return probability to those expected in metallic, insulating, or critical states. Remarkably, as we will show, these proteins exhibit properties of *critically disordered metals* without any parameter adjustment in their natural state. Their composition and geometry are self-organized into the critical state of the Anderson transition. Moreover, their fractal properties are universal and unique among critical systems since important physical quantities such as the density of states and the localization length of the wave functions fulfill "holographic" area laws, and the correlation fractal dimension appears to be precisely $d_2 = 2$.

Our investigation includes proteins from various studies[19]. A recent study on *Bacteriorhodopsin* demonstrated exceptional long-range charge transport and low activation energy, challenging common electron transport models due to unusual protein-electrode energetics and transport lengths[20]. Similarly, *Cytochrome C* proteins, essential for electron transfer, exhibited 1000 times higher conductance than single-heme or heme-free proteins and showed temperature-independent conductance, suggesting tunneling as a transport mechanism[21]. *MetMyoglobin* and *Azurin*-based junctions also displayed

temperature-independent electron transport over a wide temperature range, reinforcing the exceptional conductive properties of these proteins[18, 22]. In a single protein measurement, including a *Streptavidin* with biotin and an *Anti-Ebola Fab fragment*, conductance between electrodes attached to the proteins was in the order of nanosiemens over many nanometers, much higher than what could be explained by electron tunneling[23]. The current was mainly affected by contact resistance, so conductance for a specific path was not influenced by the distance between electrodes as long as the contact points on the protein could bridge the gap. *OmcZ* nanowires, produced by *Geobacter* species, have high electron conductivity, exceeding 30 Siemens/cm. *OmcZ* is the only known nanowire-forming cytochrome essential for forming high-current-density biofilms, which require long-distance ($\sim 10\mu\text{m}$) extracellular electron transport. Its structure[24] reveals linear and closely stacked hemes that may account for its high conductivity. We also included *Insulin* in our investigation as a reference.

Calculating the wave functions of proteins is a formidable task due to their large size, structural complexity, and the sheer number of electrons involved. Proteins comprise thousands of atoms, leading to immense atomic orbitals and interactions that must be accounted for in quantum mechanical calculations. This complexity makes high-accuracy methods, such as Density Functional Theory (DFT) or post-Hartree-Fock methods, computationally prohibitive for entire proteins, requiring significant computational resources and time. The semi-empirical extended Hückel method[25] balances computational feasibility and insightful results, making it the best option for handling the complexity of proteins within a reasonable timeframe and with available computational resources. The extended Hückel method[26] uses a linear combination of atomic orbitals (LCAO) approach. In this method, a molecular orbital Φ_n with energy ε_n is expressed as a linear combination of atomic orbitals χ_j , $\Phi_n = \sum_{j=1}^N C_{nj}\chi_j$, where N is the number of atomic orbitals. These coefficients are determined by solving the Schrödinger equation for the molecule. The atomic orbital basis is typically the Slater-type orbitals. The extended Hückel method approximates the Hamiltonian matrix elements using

$$H_{ij}^{eH} = \begin{cases} H_{ii}^{eH} & \text{for } i = j \\ K \cdot S_{ij} \cdot (H_{ii}^{eH} + H_{jj}^{eH})/2 & \text{for } i \neq j \end{cases} \quad (1)$$

where the diagonal elements H_{ii}^{eH} are the ionization energies of the atomic orbitals[26], \mathbf{S} is the overlap matrix with elements $S_{ij} = \int \chi_i(\mathbf{r})\chi_j(\mathbf{r}) d\mathbf{r}$, and K is set to 1.75. The Hamiltonian \mathbf{H}^{eH} is on a non-orthogonal basis and should be transformed into an orthogonal basis using the Löwdin transformation: $\chi'_i = \sum_{j=1}^N [S^{-1/2}]_{ij}\chi_j$, where $\mathbf{S}^{-1/2}$ is the inverse square root of the overlap matrix.

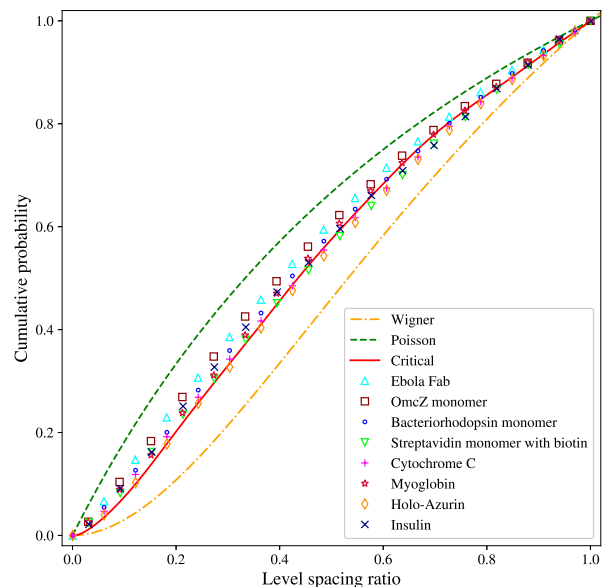


FIG. 1. Integrated level spacing ratio statistics for proteins in our investigation. The theoretical curves for Wigner random matrix theory (5) and for Poisson statistics (4) are shown. For the critical case, we used the critical value $W_c \approx 16.4$ and a cube geometry with $30 \times 30 \times 30$ sites[29] of the Anderson Hamiltonian (6). Out of the 27000 energy levels, we selected 5000 in the band center to represent $I_c(r)$ as shown.

The transformed Hamiltonian is:

$$\mathbf{H} = \mathbf{S}^{-1/2} \mathbf{H}^{eH} \mathbf{S}^{-1/2}. \quad (2)$$

Then the eigenenergies ε_n and normalized eigenvectors φ_i^n are solutions of the eigenproblem

$$\varepsilon_n \varphi_i^n = \sum_{j=1}^N H_{ij} \varphi_j^n. \quad (3)$$

The method requires the atomic coordinates of proteins as an input for computing the overlap and Hamiltonian matrices, which can be obtained, for example, from the Protein Data Bank (PDB)[27]. For the numerical calculations, we used the "Yet Another Extended Hückel Molecular Orbital Package" (YAEHMOP)[28].

Energy level statistics is one of the key methods to characterize the Anderson transition. In the study of protein level statistics, analyzing the level spacing ratio has distinct advantages over the traditional spacing distribution approach. The level spacing ratio, defined as $r_i = \min\{s_{i+1}/s_i, s_i/s_{i+1}\}$, where $s_i = \varepsilon_{i+1} - \varepsilon_i$ represents the spacing between consecutive energy levels ε_i and ε_{i+1} , provides a more robust and scale-invariant measure of level correlations. This method reduces the influence of local density variations and makes it easier to identify universal statistical properties. We introduce the integrated level spacing ratio statistics (ILSRs) as the probability that $r_i < r$ or $I(r) = \text{Prob}\{r_i < r\}$. In

the insulating phase, the energy levels are randomly distributed following Poisson statistics, and the ILSRS takes the simple form[30]

$$I_P(r) = 2r/(1+r). \quad (4)$$

The system can be characterized in the metallic phase by random matrix Hamiltonians, whose level spacings follow the Gaussian Orthogonal Ensemble (GOE) predictions well approximated by the Wigner surmise. The ILSRS can be well approximated[30] by

$$I_W(s) = 1 + \frac{2r^3 + 3r^2 - 3r - 2}{2(1+r+r^2)^{3/2}}. \quad (5)$$

In the case of the critical point of the Anderson MIT, there is no such a closed-form expression for the ILDS. Therefore, we generated a 3D Anderson Hamiltonian[6]

$$H = \sum_i W_i a_i^+ a_i - \sum_{\langle i,j \rangle} a_j^+ a_i \quad (6)$$

with nearest neighbor couplings and site energies uniformly distributed in the interval $W_i \in [-W_c/2, +W_c/2]$. The ILSRS of proteins shown in Fig.1 deviate from the Poisson and Wigner statistics, and all follow the critical Anderson curve.

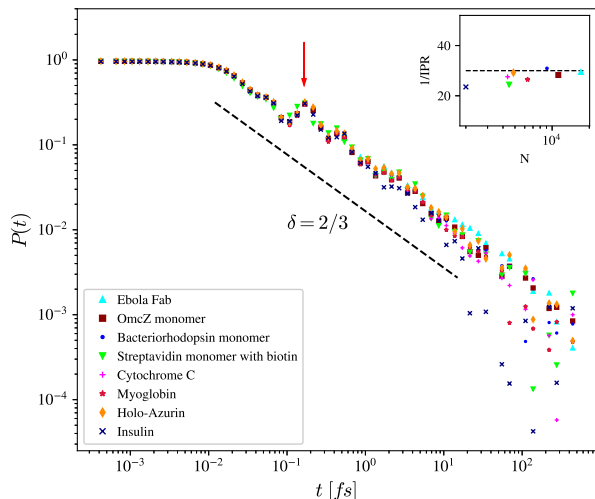


FIG. 2. The time-dependent part of the return probability for the eight proteins investigated. Notice that the curves for different proteins overlap up to about 10 fs. All curves showing power law decay consistent with $\delta \approx 2/3$. The initial part of the curve up to about 0.1645 fs corresponds to the electron diffusing within a single amino acid, where it peaks (red arrow), indicating a higher return probability due to the difficulty of leaving the initial amino acid. In the inset, the average localization length of the wave functions, i.e., $1/I_2$, the inverse of the mean IPR of the proteins, is shown as a function of their number of atomic orbitals N . The localization length is about 30 (dashed line), close to an amino acid's average number of atomic orbitals.

Another key characteristic of the critical Anderson state is the anomalous diffusion of electrons due to the fractal nature of wave functions. The anomalous nature of diffusion manifests itself in the site-averaged return probability of electrons

$$P_R(t) = \frac{1}{N} \sum_i |K_{ii}(t)|^2, \quad (7)$$

where $K_{ij}(t) = \sum_n \exp(-i\varepsilon_n t) \varphi_i^n \varphi_j^n$ is the propagator of the wave packet. This represents the likelihood that a wave packet remains at the point of its creation at $t = 0$ after a time t , or the probability that a random walker is located at its initial site at time t . It can also be expressed as a constant plus a time-dependent part $P_R(t) = I_2 + P(t)$, where the constant part is the mean inverse participation ratio (IPR) of the wave functions

$$I_2 = \frac{1}{N} \sum_{n=1}^N \sum_{i=1}^N |\varphi_i^n|^4 \quad (8)$$

and the time-dependent part

$$P(t) = 2 \sum_{n>m} C_{n,m} \cos((\varepsilon_n - \varepsilon_m)t), \quad (9)$$

is the Fourier transform of the distribution of the density-density correlation function of the eigenfunctions

$$C(\omega) = \sum_{n,m} C_{n,m} \delta(\omega - \varepsilon_n + \varepsilon_m), \quad (10)$$

where $C_{n,m} = \frac{1}{N} \sum_{i=1}^N |\varphi_i^n|^2 |\varphi_i^m|^2$ is the density-density correlation of eigenfunctions φ_i^n and φ_i^m . The decay of the return probability is characterized by the exponent δ

$$P(t) \sim t^{-\delta}. \quad (11)$$

The exponent that is $\delta = d/2$ for extended states in the metallic phase and $\delta = d_2/d$ for critical states[8] characterized by the correlation fractal dimension d_2 of the wave functions[5, 31]. In Fig.2, we show the time-dependent part of the return probability $P(t)$ for all proteins investigated. The initial part of the curve up to 0.1685 fs corresponds to the electron diffusion within a single amino acid. The bump around 0.1685 fs reflects the difficulty of leaving the initial amino acid and the higher probability of returning to the origin. The part beyond 0.1685 fs is related to the large-scale inter-amino acid diffusion. Up to the cutoff time of about 10 fs, proteins of different sizes and shapes share the same universal curve. Different proteins practically consist of the same critically disordered bulk material so that finite details of proteins don't influence the curves. The exponent $\delta \approx 2/3$ indicates that the fractal dimension of the wave functions is $d_2 \approx 2$ ($d = 3$), approximately an integer.

The distribution of density-density correlation of wave functions (10) also confirms these findings. Since the level

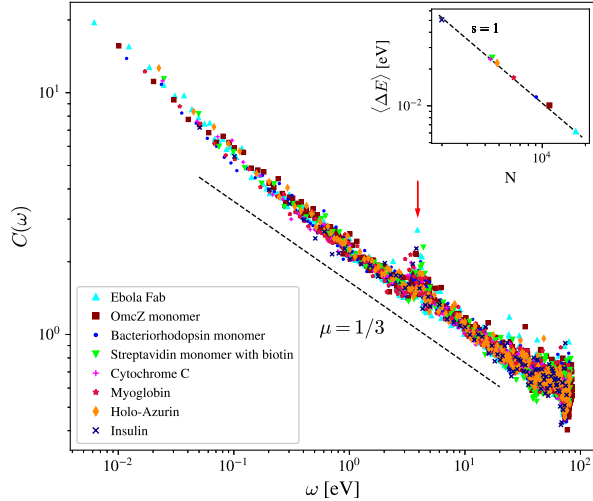


FIG. 3. Eigenfunction density-density correlation as a function of energy separation ω . $\langle \Delta E \rangle$ is the mean level spacing. Here, we can also find a peak denoted by the red arrow indicating the point $3.90 eV = \hbar/(0.1685 fs)$ corresponding to the peak of the return probability. The distribution shows power-law scaling with exponent $\mu \approx 1/3$ indicated by the dashed line. The inset shows the mean level spacing as a function of the protein size that is consistent with $\langle \Delta E \rangle \approx (105 eV)/N$ (dashed line).

spacing of proteins is highly variable throughout the energy spectrum, we can avoid unfolding the spectrum[3] and instead can study the wave function correlation between l^{th} neighbor energy levels

$$C(\omega) = \sum_{n=l+1}^N C_{n,n-l}, \quad (12)$$

where $l = n - m$, and $\omega = \langle \Delta E \rangle \cdot l$ is the mean distance between the energy levels ε_n and ε_m and we introduced the mean level spacing $\langle \Delta E \rangle = (\varepsilon_{max} - \varepsilon_{min})/N$ [32]. The correlation function is expected to show power law scaling[7, 33]

$$C(\omega) \sim \omega^{-\mu}, \quad (13)$$

with exponent $\mu = 1 - \delta$ since it is the Fourier transform (9) of the time-dependent part of the return probability. In Fig.3, we show the correlations for the investigated proteins. Up to the cutoff energy of 20 electronvolts, proteins of different sizes and shapes share the same universal curve, a power law with exponent $\mu \approx 1/3$ as we expected from the scaling of the return probability and the correlation fractal dimension $\mu = 1 - d_2/d$. The mean level spacing shows $\langle \Delta E \rangle \sim N^{-1}$ scaling following the Weyl law[34] for the Laplace-Beltrami operator, which predicts that the mean density of states $D(E)$ is proportional with \mathcal{V} , the volume of the system

$$D(E) = \langle \Delta E \rangle^{-1} \sim N \sim \mathcal{V}, \quad (14)$$

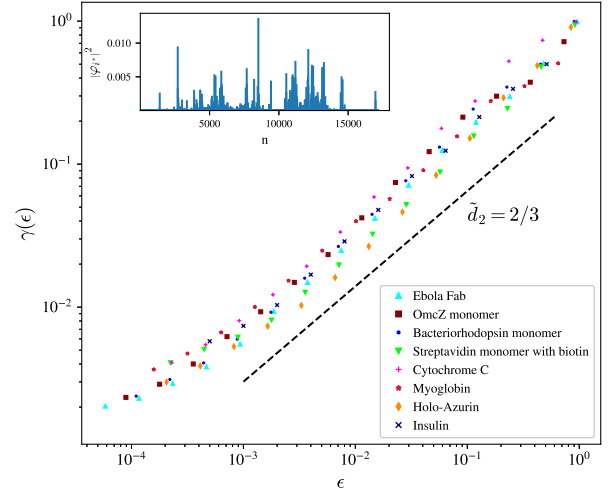


FIG. 4. Fractal dimension of the protein wave functions. The function $\gamma(\epsilon)$ defined in (15) is shown for all proteins investigated. The slope of the curve gives the dimension $\tilde{d}_2 = d_2/3$ that is consistent with $\tilde{d}_2 = 2/3$ indicated by the dashed line. The inset shows the fractal wave function $|\varphi_{i^*}^n|^2$ as a function of the index n for atomic orbital $i^* = 6234$ of the Ebola Fab protein.

which is proportional to N , the number of atomic orbitals of the proteins.

Finally, we can also directly confirm the value of the correlation fractal dimension of the wave functions. Measuring the fractal dimension in space is complicated and hampered by the intricate geometry of proteins. Calculating the fractal dimension in the energy space following Refs.[8, 35] is more straightforward. We select a site i^* for each protein for which the energy space inverse participation ratio is the smallest $\min_i \sum_n |\varphi_i^n|^4$. Then, we take boxes in the energy space so that l neighboring energies are grouped in the same box. For each box, we calculate the probability $P_k = \sum_{n=n_k}^{n_{k+1}-1} |\varphi_{i^*}^n|^2$, where $n_k = (k-1) \cdot l + 1$ is where the k^{th} box starts. We can introduce $\epsilon = l/N$ as the size of the box relative to the system size and the function

$$\gamma(\epsilon) = \sum_{k=1}^{\lfloor N/l \rfloor} P_k^2 \sim \epsilon^{\tilde{d}_2}, \quad (15)$$

where $\tilde{d}_2 = d_2/3$ in 3D ($d = 3$)[8]. In Fig.4, we show this function for all proteins investigated. It is consistent with our previous findings and confirms the value $d_2 \approx 2$.

Remarkably, the fractal dimension is nearly an integer, unlike in the Anderson model (6), where the dimension is $d_2 \approx 1.6$ [36] or in the quantum Hall system, where it is $d_2 \approx 1.43$ [5]. If we take a typical fractal wave function of the protein in real space and integrate the probability that we find the electron in a small ball of radius R , it

will scale with the surface of the ball

$$\int_{\text{ball}} d\mathbf{r} |\Phi_n(\mathbf{r})|^2 \sim R^2. \quad (16)$$

In comparison, this probability would scale with the box's volume $\sim R^3$ for a metallic conductor with extended wave functions. Scaling with the surface instead of the volume is a kind of "holographic" property[37] and probably results from evolutionary optimization towards faster electron transport[12, 13].

In conclusion, this study demonstrates that proteins naturally exist in a critical state of the Anderson metal-insulator transition, exhibiting properties of critically disordered metals without any external parameter adjustments. The unique self-organization of their composition and geometry into this critical state underlines their exceptional electron transport capabilities. These proteins defy traditional electron transport models, showing long-range, temperature-independent conductance that aligns with critical systems' fractal characteristics. Our findings suggest a profound connection between the structural complexity of proteins and their functional efficiency in biological electron transport, potentially opening new avenues for bioelectronic applications and understanding protein dynamics in complex biological systems. This critical state may also have implications for designing novel materials and devices that leverage the principles of quantum mechanics and disorder.

Acknowledgments: This research was supported by the Ministry of Culture and Innovation and the National Research, Development, and Innovation Office within the Quantum Information National Laboratory of Hungary (Grant No. 2022-2.1.1-NL-2022-00004)

* gabor.vattay@ttk.elte.hu

- [1] F. Evers and A. D. Mirlin, *Reviews of Modern Physics* **80**, 1355 (2008).
- [2] B. Altshuler, I. K. Zharekeshev, S. Kotochigova, and B. Shklovskii, *J. Exp. Theor. Phys* **67**, 625 (1988).
- [3] T. Guhr, A. Müller-Groeling, and H. A. Weidenmüller, *Physics Reports* **299**, 189 (1998).
- [4] C. Castellani and L. Peliti, *Journal of physics A: mathematical and general* **19**, L429 (1986).
- [5] W. Pook and M. Janßen, *Zeitschrift für Physik B Condensed Matter* **82**, 295 (1991).
- [6] B. Shklovskii, B. Shapiro, B. Sears, P. Lambrianides, and H. Shore, *Physical Review B* **47**, 11487 (1993).
- [7] J. T. Chalker, *Physica A: Statistical Mechanics and its Applications* **167**, 253 (1990).
- [8] B. Huckestein and L. Schweitzer, *Physical review letters* **72**, 713 (1994).
- [9] M. Feigel'Man, L. Ioffe, V. Kravtsov, and E. Cuevas, *Annals of Physics* **325**, 1390 (2010).
- [10] I. Burmistrov, I. Gornyi, and A. Mirlin, *Physical review letters* **108**, 017002 (2012).
- [11] G. S. Ng, J. Bodyfelt, and T. Kottos, *Physical review letters* **97**, 256404 (2006).
- [12] G. Vattay, S. Kauffman, and S. Niiranen, *PloS one* **9**, e89017 (2014).
- [13] G. Vattay, D. Salahub, I. Csabai, A. Nassimi, and S. A. Kaufmann, *Journal of Physics: Conference Series* **626**, 012023 (2015).
- [14] N. Amdursky, D. Marchak, L. Sepunaru, I. Pecht, M. Sheves, and D. Cahen, *Advanced Materials* **26**, 7142 (2014).
- [15] B. Zhang, W. Song, P. Pang, Y. Zhao, P. Zhang, I. Csabai, G. Vattay, and S. Lindsay, *Nano Futures* **1**, 035002 (2017).
- [16] C. D. Bostick, S. Mukhopadhyay, I. Pecht, M. Sheves, D. Cahen, and D. Lederman, *Reports on Progress in Physics* **81**, 026601 (2018).
- [17] B. Zhang and S. Lindsay, *Nano letters* **19**, 4017 (2019).
- [18] B. Kayser, J. A. Fereiro, R. Bhattacharyya, S. R. Cohen, A. Vilan, I. Pecht, M. Sheves, and D. Cahen, *The journal of physical chemistry letters* **11**, 144 (2019).
- [19] The structures of the proteins can be found in the Protein Data Bank www.rcsb.org under the following IDs: Ebola Fab 2QHR, OmcZ 7LQ5, Bacteriorhodopsin 7XJD, Streptavidin + biotin 6J6J, Cytochrome C 1HRC, Myoglobin 1MBO, Holo-Azurin 4AZU, Insulin 2HIU.
- [20] S. Bera, J. A. Fereiro, S. K. Saxena, D. Chrysikos, K. Majhi, T. Bendikov, L. Sepunaru, D. Ehre, M. Tornow, I. Pecht, *et al.*, *Journal of the American Chemical Society* **145**, 24820 (2023).
- [21] K. Garg, S. Raichlin, T. Bendikov, I. Pecht, M. Sheves, and D. Cahen, *ACS applied materials & interfaces* **10**, 41599 (2018).
- [22] S. Raichlin, I. Pecht, M. Sheves, and D. Cahen, *Angewandte Chemie* **127**, 12556 (2015).
- [23] B. Zhang, W. Song, P. Pang, H. Lai, Q. Chen, P. Zhang, and S. Lindsay, *Proceedings of the National Academy of Sciences* **116**, 5886 (2019).
- [24] Y. Gu, V. Srikanth, A. I. Salazar-Morales, R. Jain, J. P. O'Brien, S. M. Yi, R. K. Soni, F. A. Samatey, S. E. Yalcin, and N. S. Malvankar, *Nature* **597**, 430 (2021).
- [25] R. Hoffmann, *The Journal of Chemical Physics* **39**, 1397 (1963).
- [26] J. P. Lowe and K. Peterson, *Quantum Chemistry*, 3rd ed. (Elsevier Academic Press, 2006).
- [27] H. M. Berman, J. Westbrook, Z. Feng, G. Gilliland, T. N. Bhat, H. Weissig, I. N. Shindyalov, and P. E. Bourne, *Nucleic Acids Research* **28**, 235 (2000).
- [28] Greg Landrum, <https://yaehmop.sourceforge.net/> (2001).
- [29] T. Brandes, B. Huckestein, and L. Schweitzer, *Annalen der Physik* **508**, 633 (1996).
- [30] Y. Y. Atas, E. Bogomolny, O. Giraud, and G. Roux, *Physical review letters* **110**, 084101 (2013).
- [31] K. Pracz, M. Janssen, and P. Freche, *Journal of Physics: Condensed Matter* **8**, 7147 (1996).
- [32] In practice, we calculate $\langle \Delta E \rangle$ by dropping the few highest energy levels of the proteins since those are statistical outliers due to the numerical instability of the high-lying antibonding molecular orbitals.
- [33] V. Kravtsov, A. Ossipov, O. Yevtushenko, and E. Cuevas, *Physical Review B—Condensed Matter and Materials Physics* **82**, 161102 (2010).

- [34] J. Roe, *Elliptic operators, topology and asymptotic methods*, 2nd ed., Research Notes in Mathematics Series (Chapman and Hall/CRC, 1999).
- [35] R. Ketzmerick, G. Petschel, and T. Geisel, Physical review letters **69**, 695 (1992).
- [36] D. Parshin and H. Schober, Physical review letters **83**, 4590 (1999).
- [37] We borrow this wording from black hole physics, where the Bekenstein-Hawking entropy is proportional to the area of the event horizon.